

## Supplementary Information

# Colloidal micromotor in smectic A liquid crystal driven by DC electric field

Antal Jákli,\* Bohdan Senyuk, Guangxun Liao and Oleg D. Lavrentovich

Liquid Crystal Institute and Chemical Physics Interdisciplinary Program, Kent State University,  
Kent, OH 44242, USA. E-mail: jakli@lci.kent.edu

## 1 Methods

### ***Cell preparation:***

The liquid crystal (LC) octyl cyano biphenyl (8CB) with dispersed glass particles (< 0.1 volume %) was filled in the test cells in the isotropic phase by capillary action. Upon cooling the sample to the smectic A (SmA) phase, a homeotropic structure forms where the smectic layers are parallel to the substrates. This is achieved either by using homeotropic polyimide alignment coating (SE7511L and SE1211 from Nissan Chemical Industries, Ltd.), or without alignment layers, by applying a DC electric voltage higher than 4 V/ $\mu$ m (8CB is dielectrically positive with a large dielectric anisotropy  $\Delta\epsilon = 8$  at 32 °C, and the molecules are aligned parallel to the applied field). During the filling process, air voids were forced into the cell. Once equilibrated within a LC cell, the air bubbles adopt a circular shape (in the plane of the cell). Prior to the experiments, the samples were kept at room temperature for at least several hours to obtain the stationary interface profiles and director structures. The temperature of the sample was controlled with accuracy better than 0.1 °C.

### ***Optical observations:***

For Polarizing Optical Microscopy (POM), a BX60 (Olympus) microscope and Eclipse E600 (Nikon) were used. For Fluorescence Confocal Polarizing Microscopy<sup>S1,S2</sup> (FCPM) we used a custom-modified BX50 (Olympus) confocal microscope with polarization control. For FCPM observations, the LC was doped with ~0.01 % of fluorescent dye<sup>S1</sup> BTBP [*N,N'*-Bis(2,5-di-*tert*-butylphenyl)-3,4,9,10-perylenedicarboximide] (Aldrich Chemical Company, Inc.). The director structure around the particles and near the LC/air interface was analyzed using the vertical FCPM cross-section textures. The optical

contrast of the FCPM textures is determined by the intensity of the fluorescent signal, that is proportional to  $\cos^4 \beta$ , where  $\beta$  is the angle between the polarization of probing light and the local director.<sup>S1,S2</sup> The spatial resolution is about 1  $\mu\text{m}$ , worsened by birefringence of LC<sup>S1</sup> ( $\Delta n = 0.16$  at 27 °C). Because of birefringence, light scattering and some absorption, imaging conditions are better near the top bounding plate; most of our measurements were performed near the top substrates. Defocusing effects are also enhanced near the LC/air interface due to the large refractive index differences between the two media. The shape of the LC/air interface and director structures were studied at different temperatures that corresponded to the middle points of the temperature range of stability of the different phases. The electric field was applied to the inner surfaces of the bounding glass plates coated with the transparent indium tin oxide (ITO) layers and was thus perpendicular to the bounding plates.

## 2 Structural characterization

### *Shape of LC/air interface:*

The LC/air interface in the plane perpendicular to the bounding plates, as seen by FCPM, is shown in Figure S1. The interface has concave shape. The capillary length<sup>S3</sup>  $L = \sqrt{\gamma/(\rho g)}$  is of the order of 1 mm in our system; here  $\gamma \approx 0.025 \text{ J/m}^2$  is a surface tension at the LC/air interface<sup>S4</sup> and  $\rho \approx 10^3 \text{ kg/m}^3$  is the LC density,  $g = 9.8 \text{ m/s}^2$  is the acceleration due to gravity. The cell gap and thus the meniscus width are less than 0.1 mm, much smaller than  $L$ ; therefore, the effect of gravity on the meniscus profile is not substantial<sup>S4</sup> and the interface can be considered as being symmetric with respect to the midplane of the cell.

The contact angle  $\theta$  formed by the bounding plate and the LC/air interface, as measured from the FCPM textures near the triple contact line, is about  $(20 \pm 3)^\circ$  in the nematic (N) phase, between  $(20 \pm 3)^\circ$  and  $(30 \pm 3)^\circ$  in the SmA phase, for the cell thickness in the range 20  $\mu\text{m}$ -40  $\mu\text{m}$ . In the isotropic (Iso) phase,  $\theta$  increases, showing some dependence on the cell thickness:  $\theta = (45 \pm 3)^\circ$  for  $d = 20 \mu\text{m}$  and  $\theta = (28 \pm 3)^\circ$  for  $d = 40 \mu\text{m}$ .

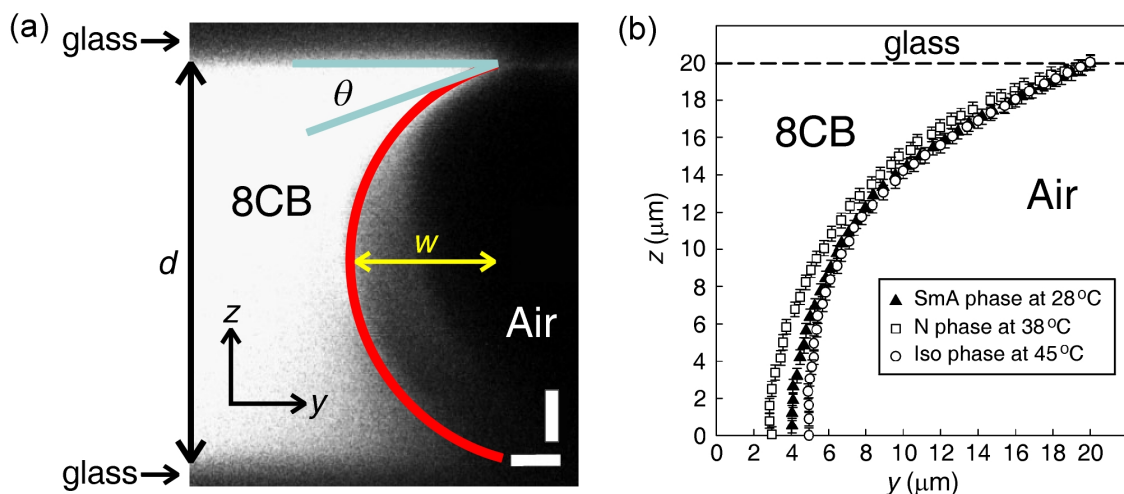


**Figure S1** The LC/air interface in a  $\sim 40 \mu\text{m}$  thick cell: (a) experimental FCPM vertical cross-section view with no polarizer; (b) the reconstructed LC/air interface profile in the same cell.  $\theta$  is an apparent contact angle,  $w$  is the width of the meniscus,  $d$  is the cell thickness. The dashed line corresponds to the top substrate and the middle of the cell is at  $z = 0$ . The error bars are determined by the FCPM resolution in the vertical direction. The horizontal and vertical bars are  $5 \mu\text{m}$ .

#### *Layer structure at liquid crystal/air interface:*

The molecules in the LC phases are anchored perpendicularly both to the solid substrates and to the air interface. Figure S2a shows the POM texture of the LC/air interface in the N phase, as viewed from above. The meniscus M appears as a wide dark band (apparently, light is deflected by the tilted LC/air interface which makes the texture dark). The director structure accommodates the surface anchoring conditions at the bounding walls and the LC/air interface through a disclination line of strength (-1/2) located in the midplane of the sample, Figure S2a, near the meniscus.<sup>55</sup> The disclination line might contain point defects-cusps.

When the N phase is cooled down into the SmA phase, the defect structures near the meniscus become more complicated, because of the layered structure of SmA. The overall shape of the meniscus is still close to the one in the isotropic and N phase, apparently because the LC/air interfacial tension  $\gamma \sim 2.5 \times 10^{-2} \text{ J/m}^2$  is still somewhat larger than the typical energy of elastic distortion in the LC, in this case represented by the energy of a wall singularity in the SmA,<sup>56</sup>  $K/\lambda \sim 10^{-2} \text{ J/m}^2$ . Here,

$K \sim 10^{-11}$  N is the Frank constant of splay and  $\lambda \sim 1$  nm is the typical molecular scale of the SmA phase, the period of the layered structure.

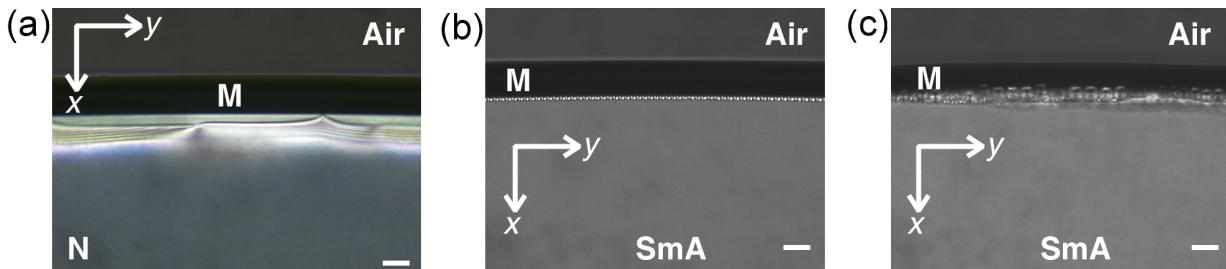


**Figure S2** POM textures of the LC/air interface: the LC/air interface in a 70  $\mu\text{m}$  thick cell in the N phase at 35  $^{\circ}\text{C}$  (a), in the SmA phase at 27  $^{\circ}\text{C}$  after cooling from the N phase with 0.5  $^{\circ}\text{C}/\text{min}$  (b) and  $\sim 5$   $^{\circ}\text{C}/\text{min}$  (c) rate between slightly uncrossed polarizers. Far from the interface the director is normal to the substrates; z-axis is normal to the page. The bar is 20  $\mu\text{m}$ .

The wedge geometry of the meniscus near the triple contact lines necessitates a formation of a Tilt Grain Boundary (TiGB), at which two systems of layers, one parallel to the plate and one parallel to the LC/air interface, are misaligned with respect to each other by the angle  $\theta_m$  that is determined by the angle between the two interfaces. According to ref. S6, depending on  $\theta_m$ , the TiGB might have a different structure. For small  $\theta_m$  (in our experiments, it corresponds to 20° - 30°), the TiGB is formed by a lattice of dislocation; no curvature defects are observed in the thinnest part of the meniscus near the triple lines. At higher values of  $\theta_m$ , the model predicts formation of an array of focal conic domains (FCDs) which is indeed observed (Fig. S2b,c and Fig. S3). These large scale domains relax the TiGB by replacing molecular scale stresses at the core of dislocations with a less energetically costly macroscopic bend of layers. The features of FCD arrays depend on the cooling rate: slower cooling results in smaller FCDs (compare parts b and c of Figure S2).

The width of the region filled with FCDs decreases with decreasing cell thickness. The FCDs are not detectable in very thin ( $< 10 \mu\text{m}$ ) films. An apparent reason is that the FCDs are macroscopic defects<sup>S6</sup> and the misalignment angle in thin samples changes too quickly for the single-FCD structure to relax the stress effectively.

Figure S3 shows the FCPM textures of the meniscus in a thick LC cell. In the vertical cross-section, FCPM distinguishes the FCD-free region (indicated by two arrows) formed by two differently

oriented domains that are separated by a sharp TiGB that extends to the triple contact line. The FCPM texture clearly reveals the misalignment of the two domains. The top domain “1” in Figure S3 has a vertical director orientation and thus produces a weaker fluorescence signal than the bottom domain

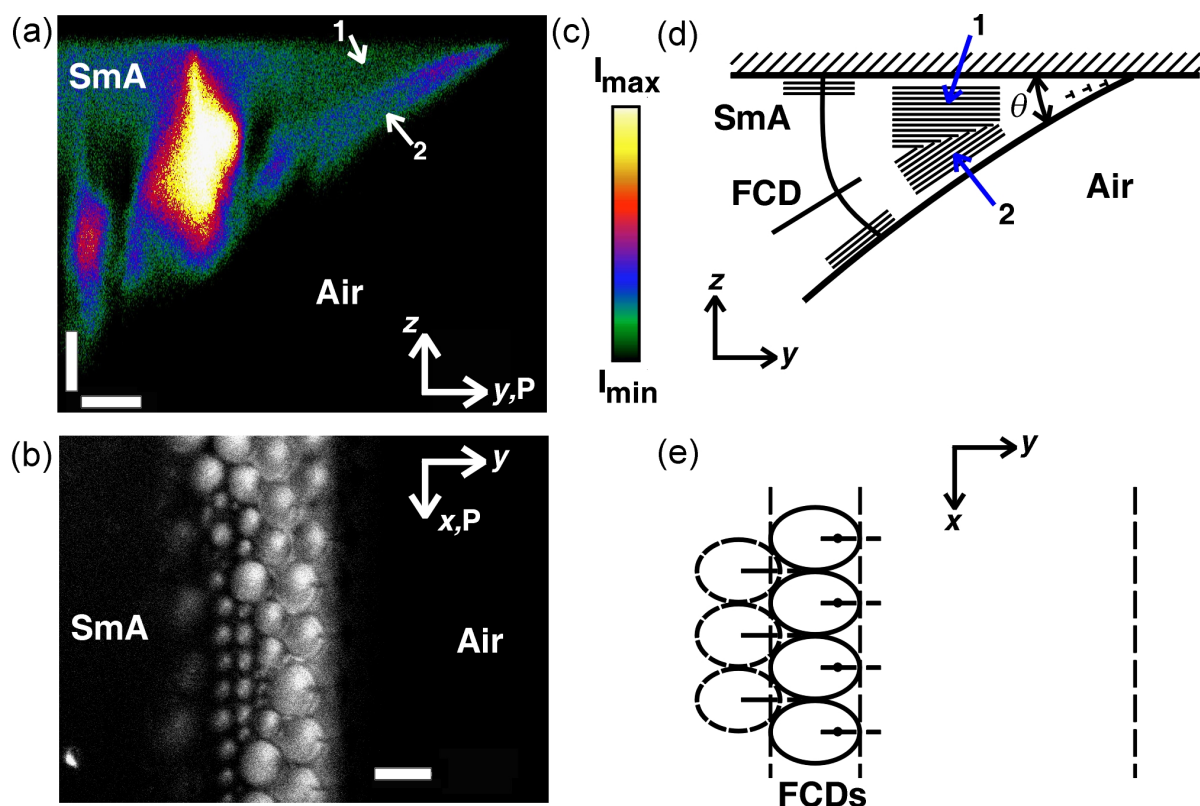


**Figure S3** (a) Vertical cross section ( $zy$ ) and (b) in-plane ( $xy$ ) views of the defect structures at the SmA/air interface. (a,b) FCPM pictures of the LC/air interface in 70  $\mu\text{m}$  thick cell in the SmA phase at 27  $^{\circ}\text{C}$  along the vertical plane (a) and in-plane (b). Far from the contact line arrays of focal conic domains develop in the thicker part of the meniscus; the focus is in the FCDs’ plane. “P” shows the direction of light polarization in FCPM. (c) Color bar shows the FCPM color-coded intensity scale. (d) and (e) Schematic diagrams of smectic FCPM textures in (a) and (b). The horizontal and vertical bars are 10  $\mu\text{m}$ .

“2”, in which the director is titled by an angle  $\theta$  (despite the fact that the top domain “1” is closer to the impinging plane). Although the individual dislocations are not resolved in Figure S3, some of them (of a large Burgers vector) can be sometimes observed in the  $xy$  view of the POM and FCMP images. The dislocation part of the TiGB is located in the deep SmA bulk, which indicates that both the surface

tension  $\gamma$  of the LC/air interface and the polar surface anchoring at the rigid wall are larger than  $K/\lambda$  (see refs S7, S8).

**Solid spherical particles in the smectic liquid crystal:**

A foreign inclusion inserted into the LC bulk causes distortions such as tilt, bend and dilation of the smectic layers in SmA phase, or bend, twist and splay of the director in the N phase. The surface of glass particles aligns the director tangentially.<sup>S9</sup> This tangential anchoring results in a bipolar smectic texture with two singular lines emanating from the poles of the spheres and parallel to the unperturbed director in the far field<sup>S9,S10</sup> (Fig. S4). In the thick cells, the vertical FCPM views of the samples

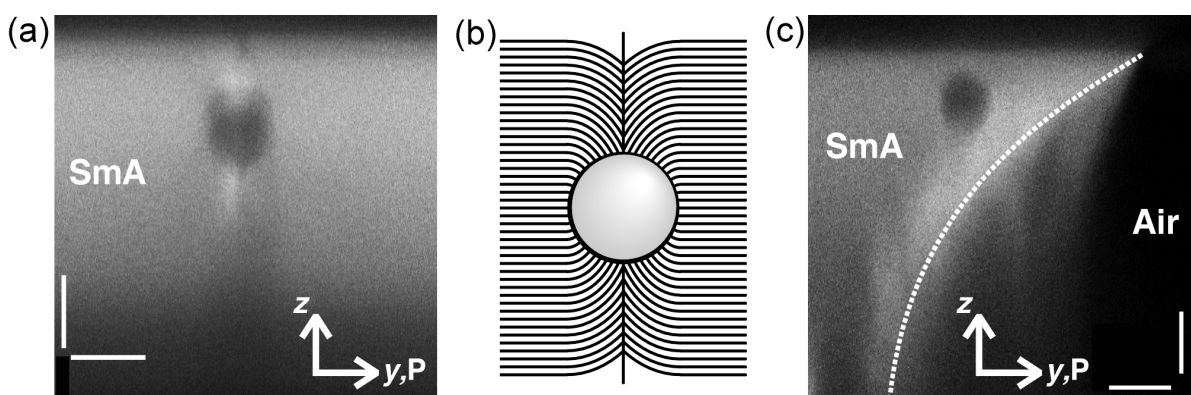


**Figure S4** Smectic layers distortions around a spherical particle with layers parallel to the substrates: (a) vertical FCPM images of the defect structure around the spherical particles in the SmA phase in a cell with  $d \sim 25 \mu\text{m}$ . (b) Model structure of the smectic layers around a particle with planar anchoring condition. Lines represent the smectic layers. The liquid crystal molecules are normal to the layers. (c) The position of a solid particle at the LC/air interface in the SmA phase in a  $60 \mu\text{m}$  thick cell near the focal conic domains. Dotted line outlines the actual boundary. “P” shows the direction of light polarization in FCPM. The horizontal and vertical bars are  $5 \mu\text{m}$ .

reveal that the glass spheres “levitate” in the bulk of the cell, despite the fact that their density is about twice the density of 8CB. This levitation is caused by the elastic nature of the SmA. As easy to see from Figure S4b, the smectic layers are strongly curved near the poles of the spheres. The sphere would thus elastically repel from the substrates at which the SmA layers are flat. The spheres appear to

be neutrally buoyant; FCPM textures demonstrate that the particles can be located practically anywhere in the cell. The gravity force is on the order of  $\frac{4}{3}\pi a^3 \Delta \rho g \sim 0.6 \text{ pN}$ , while the elastic force might be on the order of Frank constant<sup>s11</sup>  $K \sim 10 \text{ pN}$ . In cells thinner than  $20 \mu\text{m}$ , the particles are also levitating, although we observe that they tend to accumulate closer to the boundaries than to the middle of the cell. Nonetheless, the top and the bottom parts of the cell contain about equal numbers of particles, suggesting again that their locations are determined mainly by the elastic forces. The balance of forces might be different in thin cells as compared to thick cells, because some of the spheres do not carry the vertical singular lines shown in Figure S4b; the latter implies that the tangential orientation at the spherical surface is violated. In many instances, a gap between the substrates and the spheres is clearly visible in thin cells, in other instances, it cannot be resolved by FCPM.

Figure S4c shows a spherical particle in the narrow triangular region confined between the glass wall and the SmA/air interface. Note that there are no defect lines emanating from the poles of the sphere. The particle is clearly levitating in the bulk, in the region of TiGB. The particle remains distant from the LC/air interface. Location of the particle at the TiGB region can be explained by the elastic trapping: A sphere replaces a portion of the TiGB and thus decreases the energy of the system by  $\sim a^2 K / \lambda$ , where  $\lambda$  is the molecular scale of the SmA phase that can also be understood as the core size of an elementary dislocation. Note that there is no long-range interaction between the particles and the TiGB: the particles need to approach the TiGB (as a result of Quincke rotation and corresponding translation, for example) to be trapped at it.

Above the SmA-N phase transition temperature, the TiGB disappears because the director distortions spread over macroscopic scales (on the order of the local thickness of the LC in the meniscus region). The glass spheres move away from the LC/air interface. In the N phase, a single (-1/2) disclination line with point defects forms along the N/air interface, near the midplane of the cell.<sup>s5</sup> In some instances, the drift of point defects drags some of the remaining glass spheres along the N/air interface; however, this motion is much slower than the orbiting motion of the spheres rotating in the applied electric field when the LC is in the SmA phase.

## References

- S1. I. I. Smalyukh, S. V. Shiyanovskii and O. D. Lavrentovich, *Chem. Phys. Lett.*, 2001, **336**, 88-96.
- S2. S. V. Shiyanovskii, I. I. Smalyukh and O. D. Lavrentovich, in *Defects in Liquid Crystals: Computer Simulations, Theory and Experiments*, ed. O. D. Lavrentovich, P. Pasini, C. Zannoni, and S. Zumer, NATO Science Series, II: Mathematics, Physics and Chemistry, Kluwer Academic Publishers, Dordrecht, 2001, **43**, 229-270.
- S3. A. W. Adamson and A. P. Gast, *Physical chemistry of surfaces*, New York: Wiley, 6th edn., 1997.
- S4. J.-Ch. Géminard, R. Holyst and P. Oswald, *Phys. Rev. Lett.*, 1997, **78**, 1924-1927.
- S5. J. Ignes-Mullol, J. Baudry, L. Lejcek and P. Oswald, *Phys. Rev. E*, 1999, **59**, 568-577; J. Ignes-Mullol, J. Baudry and P. Oswald, *Phys. Rev. E*, 2001, **63**, 031701; J. Ignes-Mullol, L. Scurtu and P. Oswald, *Eur. Phys. J. E*, 2003, **10**, 281-288.
- S6. M. Kleman and O. D. Lavrentovich, *Eur. Phys. J. E*, 2000, **2**, 47-57.
- S7. L. Lejcek and P. Oswald, *J. Phys. II (France)*, 1991, **1**, 931-938.
- S8. I. I. Smalyukh and O. D. Lavrentovich, *Phys. Rev. Lett.*, 2003, **90**, 085503.
- S9. G. Liao, I. I. Smalyukh, J. R. Kelly, O. D. Lavrentovich and A. Jákli, *Phys. Rev. E*, 2005, **72**, 031704; preprint posted in Electronic Liquid Crystals Communications, [http://www.elc.org/docs/2005\\_02\\_25\\_10\\_57\\_49](http://www.elc.org/docs/2005_02_25_10_57_49).
- S10. C. Blanc and M. Kleman, *Eur. Phys. J. E*, 2001, **4**, 241-251.
- S11. O. P. Pishnyak, S. Tang, J. R. Kelly, S. V. Shiyanovskii and O. D. Lavrentovich, *Phys. Rev. Lett.*, 2007, **99**, 127802.